Power Electronic Systems
Laboratory

IEEE Transactions on Power Electronics, Vol. 37, No. 9, pp. 10086-10090, September 2022

New Return-Path-Inductor Buck-Boost Y-Inverter Motor Drive with Reduced Current Stresses

D. Menzi,
J. Huber,
L. Kappeler,
G. Zulauf,
J. W. Kolar

Eidgenössische Technische Hochschule Zürich
Swiss Federal Institute of Technology Zurich

This article has been accepted for publication in IEEE Transactions on Power Electronics. This is the author's version which has not been fully edited and content may change prior to final publication. Citation information: DOI 10.1109/TPEL.2022.3163465

New Return-Path-Inductor Buck-Boost Y-Inverter Motor Drive with Reduced Current Stresses

David Menzi, *Student Member, IEEE,* Jonas E. Huber, *Member, IEEE,* Lorenz Kappeler, Grayson Zulauf, Johann W. Kolar, *Fellow, IEEE*

***Abstract*—Variable Speed Drives (VSDs) for electric motors are a foundational component of global electrification, with electric motors consuming 45% of global electricity. Conventional three-phase buck-boost inverter topologies have substantial low-frequency current stresses in the buck-boost inductor, driving size, losses, and cost in VSD systems. In this Letter, we propose a novel circuit topology for phase-modular three-phase buck-boost inverter systems based on the four-switch non-inverting buck-boost concept, which we call the Return-Path-Inductor Y-Inverter (RPI-YI). By relocating the buck-boost inductors from the forward current path to the return path, the RPI-YI concept reduces the inductor RMS and peak current stresses by up to 90 % compared to a conventional topology, resulting in a potential magnetics volume reduction of 80 %. The RPI-YI concept, therefore, supports more compact, efficient realizations of modular buck-boost VSD systems.**

***Index Terms*—Three-Phase Buck-Boost Inverter, Y-Inverter, Return-Path Inductor, Wide Input and Output Voltage Range**

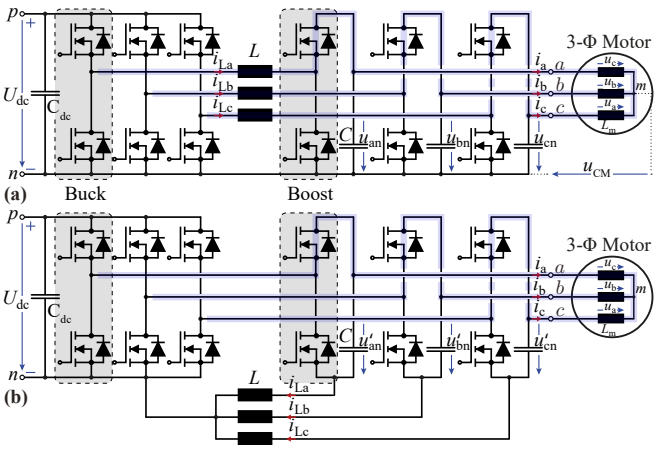

Fig. 1. Main power circuit topology of **(a)** standard Forward-Path-Inductor Y-Inverter (FPI-YI), as well as **(b)** proposed novel Return-Path-Inductor Y-Inverter (RPI-YI) Variable Speed Drive (VSD). The motor current paths in buck operation are highlighted in light blue.

I. Introduction

Variable Speed Drives (VSDs) for electric motors are a critical element of the infrastructure that supports broad electrification [1,2], with electric motors and their drives currently accounting for 45 % of the world's total electricity usage [3]. The existing and increasing ubiquity of electric motors demands VSDs that feature a wide operating range and are efficient, cost-effective, power-dense, and tightly integrated.

For VSD applications that require motor drive voltages both above and below the DC-link voltage, the state-of-the-art topology is the Forward-Path-Inductor Y-Inverter (FPI-YI), which is shown in **Fig. 1a** [4]–[8]. This inverter structure is phase-modular, features a low number of magnetic components, and has mutually exclusive, i.e., quasi-single-stage buck and/or boost High-Frequency (HF) conversion in each module. The FPI-YI converts a dc input voltage U_{dc} into strictly positive output capacitor voltages u_{an}, u_{bn}, u_{cn} of arbitrary amplitude below and above U_{dc}. An offset voltage u_{CM} is present in all three output capacitor voltages, and therefore does not drive a current into the open-star-point motor windings. Accordingly, sinusoidal motor phase voltages u_{a}, u_{b}, u_{c} (with amplitude $\hat{U}_{\mathrm{ac}}$ and low HF content due to the output capacitor of each module) and currents i_{a}, i_{b}, i_{c} (with amplitude $\hat{I}_{\mathrm{ac}}$) are applied to the motor.

The primary drawback of the conventional FPI-YI topology is that the buck-boost inductor in each stage, L, is subject to high Low-Frequency (LF) current stresses, especially for high modulation indices $M = 2\hat{U}_{\mathrm{ac}}/U_{\mathrm{dc}}$, where the peak LF current is given by $\hat{I}_{\mathrm{L}} = \hat{I}_{\mathrm{ac}} \cdot \max(1, M)$ — an LF current stress that is strictly larger than the motor current (see Fig. 3a). This buck-boost inductor, therefore, drives cost, size, losses, and design complexity in such FPI-YI VSD systems.

We propose a novel topology to reduce these LF current stresses, drawing inspiration from literature that relocates inductors of a DC/DC buck converter to lower current stress [9]. The proposed Return-Path-Inductor Y-Inverter (RPI-YI) concept is shown in **Fig. 1b**, where the buck-boost inductor L is relocated to the return path to dramatically lower the LF current stress. The RPI-YI concept maintains the critical properties of the FPI-YI topology — most notably, phase modularity and buck-boost capabilities — but the peak LF current stresses are now given by $\hat{I}_{\mathrm{L}} = \hat{I}_{\mathrm{ac}} \cdot (\max(1, M) - 1)$, a dramatic reduction relative to the FPI-YI current stresses (see Fig. 3b). The symmetric three-phase load currents i_{a},i_{b},i_{c} sum to zero in the motor winding star-point, flowing from one phase to another without introducing any LF inductor currents in buck operation (cf., **Fig. 1**) and substantially reducing current stresses in boost operation. While inductor-less buck-boost inverter topologies exist in literature (e.g., [10]), eliminating the buck-boost inductor entirely comes at the cost of an increased number of active components, limited load angle ranges, and the need for three capacitive LF energy storage elements. As a topology candidate, then, the RPI-YI is conceptually positioned between an FPI-YI, with large magnetics volume and stresses, and these fully inductor-less buck-boost inverters, with the limitations outlined above.

In this Letter, we detail the RPI-YI operating principle (**Section II**), briefly discuss the control structure (**Section III**), and verify the dramatic reduction in inductor current stresses in a hardware demonstrator (**Section IV**) before concluding the paper in **Section V**.

This article has been accepted for publication in IEEE Transactions on Power Electronics. This is the author's version which has not been fully edited and content may change prior to final publication. Citation information: DOI 10.1109/TPEL.2022.3163465

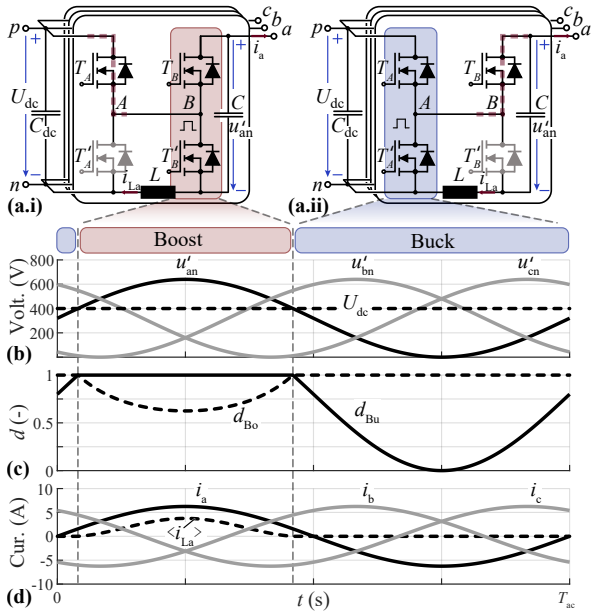

Fig. 2. Operating concept of the RPI-YI, highlighted for phase module a. **(a.i)** boost operation ($u'_{\mathrm{an}} > U_{\mathrm{dc}}$) and **(a.ii)** buck operation ($u'_{\mathrm{an}} \leq U_{\mathrm{dc}}$). **(b)** DC input voltage U_{dc} and output capacitor voltage waveforms $u'_{\mathrm{an}}, u'_{\mathrm{bn}}, u'_{\mathrm{cn}}$ for a constant CM offset voltage, i.e., sinusoidally shaped phase-module output voltages. **(c)** Duty cycles of the module a buck half-bridge d_{Bu} and of the boost half-bridge d_{Bo}. **(d)** Motor currents $i_{\mathrm{a}}, i_{\mathrm{b}}, i_{\mathrm{c}}$ and LF buck-boost inductor current $\langle i_{\mathrm{La}} \rangle$.

II. RPI-YI Operating Principle

The operating principle of the RPI-YI can be characterized by a single module, since each phase is operated independently. The circuit of phase module a under RPI-YI operation for buck and boost mode are shown in **Fig. 2a.i** and **a.ii**, respectively, with the output capacitor voltage waveforms u'_{an}, u'_{bn}, u'_{cn} shown in **Fig. 2b** under Sinusoidal Pulse-Width Modulation (SPWM) operation (that is, with a minimum constant offset voltage $u'_{\mathrm{CM}} = \hat{U}_{\mathrm{ac}}$).

The operating mode (buck or boost) depends on the instantaneous modulation index, i.e.,

$$\begin{aligned} m(t) &= u'_{\mathrm{an}}/U_{\mathrm{dc}} = M(1+\sin(\omega t)), \\ M &= 2\hat{U}_{\mathrm{ac}}/U_{\mathrm{dc}}, \end{aligned} \tag{1}$$

where ω denotes the angular frequency of the output voltage.

For $m(t) > 1$ ($u'_{\mathrm{an}} > U_{\mathrm{dc}}$), phase module a operates instantaneously in boost mode (**Fig. 2a.i**). In this mode, the high-side switch of the buck bridge-leg T_{A} is on (connecting node A to the positive DC-link rail p) and the boost half-bridge (T_{B}, T'_{B}) regulates the output voltage. In this configuration, the inductor remains in the LF path and incurs a LF current component $\langle i_{\mathrm{La}} \rangle$ in addition to the HF current ripple.

For $m \leq 1$ ($u'_{\mathrm{an}} \leq U_{\mathrm{dc}}$), phase module a operates instantaneously in buck mode, as shown in **Fig. 2a.ii**. The high-side switch of the boost bridge-leg T_{B} is kept on, continuously connecting node B to the output terminal a, and the buck half-bridge (T_{A}, T'_{A}) is switched to regulate the output voltage. In the RPI-YI configuration, the output capacitor C acts as a DC (and LF AC) block, and the inductor does not conduct any LF current. The AC output current is returned via the other two motor phases (cf., **Fig. 1**). The RPI-YI inductor does still incur an HF Voltage-Time Area (VTA) and therefore an HF current ripple, which can be used to decrease the hard-switching losses of the power semiconductors or even to achieve full soft-switching [11,12].

The duty cycles for mutually exclusive operation of the buck and boost half-bridges are shown in **Fig. 2c**, with identical duty cycles to the FPI-YI [5] that are set dependent on the instantaneous modulation index of (1) as

$$d_{\mathrm{Bu}}(t) = \min(1, m(t)), \tag{2}$$

$$d_{\mathrm{Bo}}(t) = \min(1, 1/m(t)), \tag{3}$$

where d_{Bu} and d_{Bo} denote the duty cycles of the buck and boost half-bridge, respectively.

In both operating modes, the output terminal voltage (relative to the negative DC-link rail u_{an}) is the sum of the continuous output capacitor voltage u'_{an} and the buck-boost inductor voltage u_{La}, which includes an HF voltage component. Therefore, an inductive load (for example, provided by the winding inductance L_{m} of the electric machine, cf., **Fig. 1b**) is required for the RPI-YI to operate with a sinusoidal output current. However, with typical motor inductance values L_{m} in the mH-range (i.e., $L_{\mathrm{m}} >> L$), the resulting HF motor current variation caused by the RPI-YI remains small compared to the HF current ripple in the buck-boost inductor L. Also, no LF motor current harmonic distortion occurs. Note that this limitation to inductive loads does not apply to the traditional FPI-YI configuration; the FPI-YI would allow to impress sinusoidal output currents also into purely ohmic loads.

A. Magnetics Volume Assessment

The time-varying LF local average (within one switching cycle) inductor current $\langle i_{\mathrm{La}} \rangle$ is found by balancing the output capacitor C charge in periodic steady-state operation, and is dependent on the boost half-bridge duty cycle $d_{\mathrm{Bo}}(t)$:

$$\langle i_{\mathrm{La}} \rangle(t) = \frac{i_{\mathrm{a}}(t)(1-d_{\mathrm{Bo}}(t))}{d_{\mathrm{Bo}}(t)}. \tag{4}$$

The LF inductor current is, therefore, zero in buck operation ($d_{\mathrm{Bo}}(t) = 1$, see in **Fig. 2c,d**) and is significantly reduced compared to FPI-YI current stresses.

More generally, the LF FPI-YI and RPI-YI buck-boost inductor current stresses are compared across modulation index M (see (1)) in **Fig. 3** (normalized against AC output current), where I_{L} and $\hat{I}_{\mathrm{L}}$ represent the (global) RMS and peak value of $\langle i_{\mathrm{La}} \rangle$, respectively, within one fundamental period. The proposed RPI-YI approach has a significant reduction in both RMS and peak current stresses in both buck and boost operation across the entire modulation index M. This dramatic reduction occurs because the three-phase motor currents are summing to zero in the motor starpoint, and therefore, in buck operation no LF current returns via the RPI-YI inductor ($I_{\mathrm{L}} = 0\,\mathrm{A}$).

For a given operating point and switching frequency, the HF VTA applied to the buck-boost inductors is identical for

This article has been accepted for publication in IEEE Transactions on Power Electronics. This is the author's version which has not been fully edited and content may change prior to final publication. Citation information: DOI 10.1109/TPEL.2022.3163465

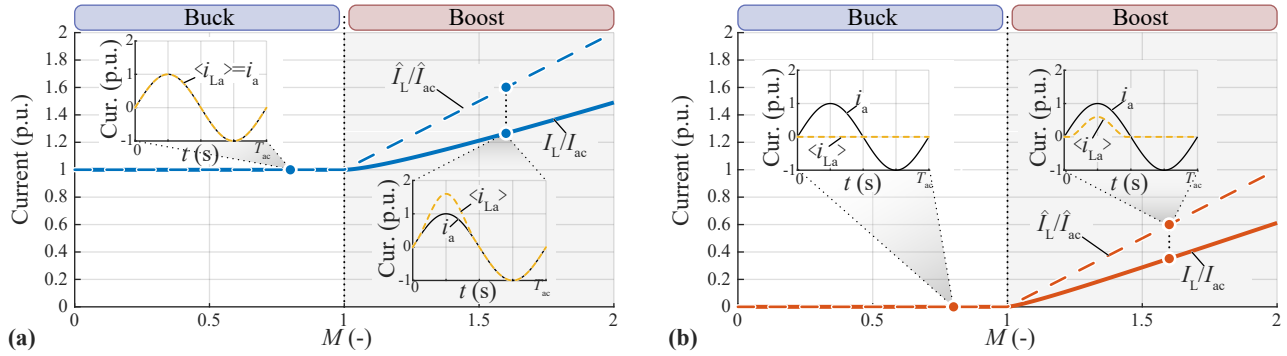

Fig. 3. LF RMS and peak current stresses of the buck-boost inductor L under **(a)** conventional FPI-YI operation and **(b)** the proposed RPI-YI concept. Values are normalized to the RMS and peak AC motor current over the modulation index $M = 2\hat{U}_{ac}/U_{dc}$. LF current waveforms are highlighted for $M = 0.8$ and $M = 1.6$.

FPI-YI and RPI-YI, and when selecting identical inductance values L, the inductor area product is [13]

$$AP \propto L\hat{I}_L I_L. \tag{5}$$

Assuming a maximum $M = 1.6$, this area product is reduced by 90 % for the proposed RPI-YI configuration over the conventional FPI-YI. With the volume of an inductor scaling approximately with $AP^{\frac{3}{4}}$ [14], this corresponds to a reduction in the inductor volume of ≈80 % compared to the conventional FPI-YI.

B. Converter Loss Considerations

In order to allow a performance estimate for an RPI-YI system the main converter loss components are compared qualitatively to an FPI-YI in the following:

- **Semiconductors:** Given $L_m >> L$ (i.e., negligible HF motor current variation), the buck and boost semiconductor switched voltages and the conducted HF and LF currents of RPI-YI and FPI-YI are identical for a given operating point. Hence, identical semiconductor switching and conduction losses can be expected.
- **Capacitors:** Both DC-link C_{dc} and AC-side capacitors C (given $L_m >> L$) of RPI-YI and FPI-YI are subject to identical HF current stresses and accordingly the same capacitor losses.
- **Inductors:** As discussed in **Section II-A**, the buck-boost inductors L of RPI-YI and FPI-YI are subject to the same HF VTA, such that (neglecting the impact of the LF premagnetization) identical HF inductor losses can be expected. In contrast, the LF conduction losses of the RPI-YI inductors are substantially reduced compared to the FPI-YI.

Based on this component stress assessment, RPI-YI efficiency values very similar to the FPI-YI can be expected (with reported FPI-YI efficiency values $> 98\,\%$ [7,8]), with the main advantage of the RPI-YI magnetics volume reduction.

III. Control

While control is not the primary topic of this Letter, we include a brief discussion of a possible control structure for the proposed RPI-YI topology for completeness, with a graphical overview shown in **Fig. 4**.

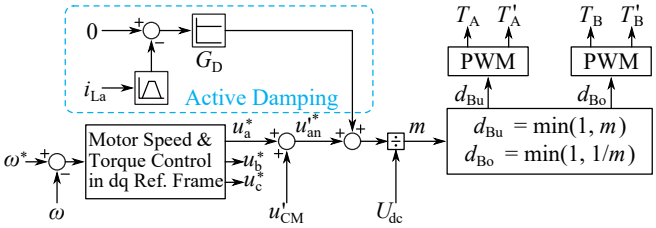

Fig. 4. Example RPI-YI control concept. The active damping is not required but allows for aggressive motor current control without introducing ringing in the buck-boost inductor currents.

The RPI-YI topology applies the switched Pulse-Width Modulation (PWM) voltages directly to the motor, so a standard motor control algorithm for a buck-type voltage source inverter can be utilized (with the additional buck-boost functionality enabling $m(t) > 1$). Note that this is a major difference from the standard FPI-YI, where the motor currents must be controlled by adjusting the output capacitor voltages [5]).

The speed and torque controller—typically in the d-q reference frame—seeks to drive the difference between the angular speed reference ω^* and the measured value ω to zero by selecting the appropriate motor phase voltage references u_a^*, u_b^*, u_c^* in order to impress according torque generating currents in the motor stator windings. The desired LF capacitor voltage reference (here, for module a) is calculated by adding the appropriate Common Mode (CM) offset voltage value u'_{CM}, and this voltage reference is, in the end, translated into a modulation index m_a (through (1)) and duty cycles d_{Bu}, d_{Bo} (through (2)).

The inductor current in the RPI-YI L does not necessarily need to be controlled (the LF current $\langle i_{La} \rangle(t)$ displayed in **Fig. 2d** results naturally in open-loop operation), but ringing may occur if the motor current control is aggressive. To avoid this ringing and support a high-bandwidth control regime, active damping can be introduced, as shown in **Fig. 4**, where the HF content of i_{La} (i.e., with reference value equal to zero) is directly regulated through a correction term that is added to the output capacitor voltage reference value. Alternatively, the fully-cascaded control structure proposed in [5] could be used for the RPI-YI, with the innermost controller regulating either the buck-boost inductor current or the current between the nodes A and B (see **Fig. 2**).

This article has been accepted for publication in IEEE Transactions on Power Electronics. This is the author's version which has not been fully edited and content may change prior to final publication. Citation information: DOI 10.1109/TPEL.2022.3163465

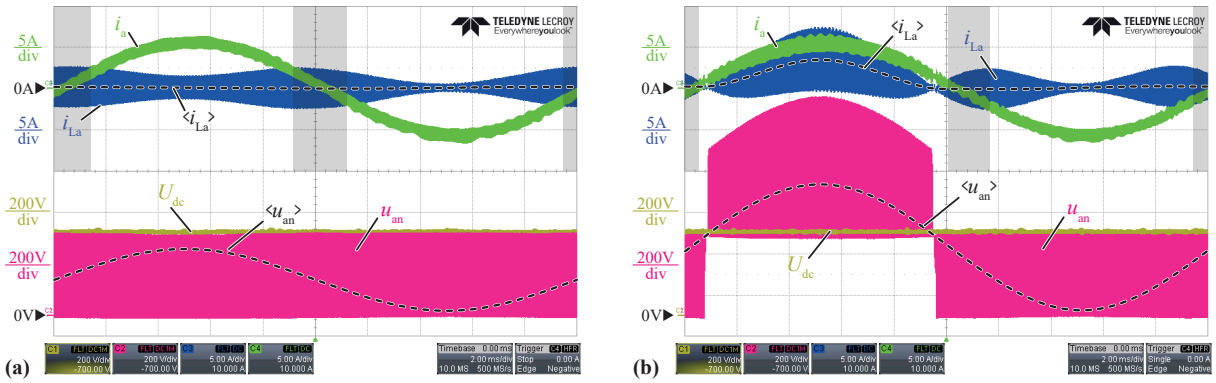

Fig. 5. RPI-YI experimental waveforms: DC input voltage U_{dc}, module a terminal output voltage with respect to the negative DC-link rail u_{an}, AC output current i_{a}, and buck-boost inductor current i_{La}. Both operating points were recorded with $U_{\mathrm{dc}} = 400\,\mathrm{V}$ and $\hat{I}_{\mathrm{ac}} = 5.5\,\mathrm{A}$, with **(a)** $M = 0.8$ ($P = 1.7\,\mathrm{kW}$) and **(b)** $M = 1.6$ ($P = 3.3\,\mathrm{kW}$). The LF buck-boost inductor current $\langle i_{\mathrm{La}} \rangle$ and output voltage $\langle u_{\mathrm{an}} \rangle = u'_{\mathrm{an}}$ were extracted from the exported oscilloscope waveforms and added on top of the screenshot as dashed lines, for illustration purposes. Regions of the fundamental period where the semiconductor current direction inverts within one switching period (where zero-voltage-switching could be achieved) are highlighted in light grey.

TABLE I
RPI-YI PROTOTYPE SPECIFICATIONS

Parameter	Value
System power P_{nom}	3.3 kW
DC input voltage U_{dc}	400 V
AC pk. voltage $\hat{U}_{\mathrm{ac}}$	160 V_{pk} / 320 V_{pk}
AC frequency f_{ac}	50 Hz
Switching frequency f_{s}	100 kHz
DC-link capacitor C_{dc}	60 µF
Buck-boost inductor L	220 µH
Capacitor C	2.2 µF
Load inductor L_{m}	2.8 mH
Load resistor	25 Ω/50 Ω

IV. Experimental Verification

The proposed RPI-YI concept is validated with a hardware demonstrator system, built according to the specifications shown in **Table I** (component designators refer to **Fig. 1b**) and with 1.2 kV Silicon Carbide (SiC) MOSFETs as the bridge-leg power semiconductors. An inductive-resistive three-phase load (i.e., operation close to unity power factor as it is typical for permanent magnet synchronous machines [7]) is driven from a DC input voltage of $U_{\mathrm{dc}} = 400\,\mathrm{V}$ and the RPI-YI inverter is operated with open-loop control.

Fig. 5a shows the measured operating waveforms during buck-mode operation at $M = 0.8$, $\hat{I}_{\mathrm{ac}} = 5.5\,\mathrm{A}$, and $P = 1.7\,\mathrm{kW}$. The inverter generates a sinusoidal AC output current i_{a}, and the terminal a output voltage (relative to the negative DC-link rail) u_{an} remains strictly below U_{dc}, as it must under buck operation. The LF output voltage component $\langle u_{\mathrm{an}} \rangle \approx u'_{\mathrm{an}}$ is extracted from the captured oscilloscope data and added to **Fig. 5a** for completeness. Most importantly for the verification of the RPI-YI concept, the buck-boost inductor current i_{La} has zero LF component $\langle i_{\mathrm{La}} \rangle = 0$, as expected.

Operation in boost mode is shown in **Fig. 5b**, with $M = 1.6$, $\hat{I}_{\mathrm{ac}} = 5.5\,\mathrm{A}$, and $P = 3.3\,\mathrm{kW}$. Here, during the first half of the cycle, the converter operates in a boost mode with u_{an} above U_{dc}, and the buck-boost inductor incurs an LF current $\langle i_{\mathrm{La}} \rangle > 0$ when $m(t) > 1$.

TABLE II
RPI-YI LF CURRENT STRESSES

Op.	Param.	Calc.	Meas.	Error
$M = 0.8$	$I_{\mathrm{L}}/I_{\mathrm{ac}}$	0.0	0.03	-
	$\hat{I}_{\mathrm{L}}/\hat{I}_{\mathrm{ac}}$	0.0	0.04	-
$M = 1.6$	$I_{\mathrm{L}}/I_{\mathrm{ac}}$	0.35	0.38	+8.6 %
	$\hat{I}_{\mathrm{L}}/\hat{I}_{\mathrm{ac}}$	0.60	0.64	+6.7 %

These measured current stresses for the RPI-YI buck-boost inductor are compared to the analytical values in **Table II,** with the RMS and peak currents normalized to the AC output current. The measured values are close to those predicted by **Fig. 3**, with slightly higher measured stresses due to *(a)* a selected offset voltage of $u'_{\mathrm{CM}} = 105\,\%\,\hat{U}_{\mathrm{ac}}$ for a practical realization and *(b)* non-zero LF capacitive reactive currents from the output capacitor C returning via the buck-boost inductor.

Nonetheless, the predicted RPI-YI operation matches the measured results closely, validating the dramatic reduction in LF current inductor stress for the proposed RPI-YI approach.

V. Conclusion

VSDs are a critical component to the widespread electrification of industry, logistics, and mobility. In this Letter, we propose a new topology and operating concept to reduce the largest passive component in buck-boost inverter drives, the inductor. The Return-Path-Inductor Y-Inverter (RPI-YI) concept moves this buck-boost inductor from the forward path (conventional, or Forward-Path-Inductor Y-Inverter (FPI-YI)) to the return path, reducing the LF current stresses by up to 90 % considering a typical operating range. We explain the basic operating principles of the RPI-YI topology, derive an analytical current stress comparison between the RPI-YI

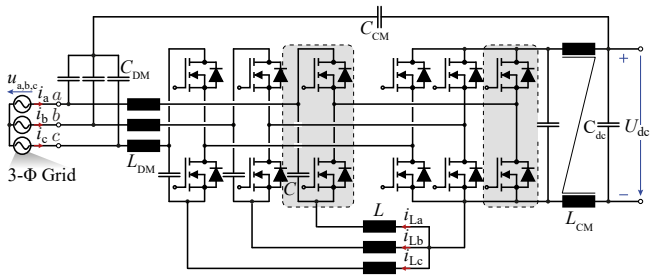

Fig. 6. Three-phase PFC rectifier application of the proposed novel Return-Path-Inductor Y-converter, i.e., RPI Y-Rectifier (RPI-YR). The power circuit depicted here includes a CM output filter with internal CM capacitor filter path as described in [15] ensuring a constant ground potential of the DC output voltage, which is crucial for series connected converter stages [16]. It is important to note that the CM inductor can be either located on the DC side (as shown) or on the AC side of the converter switching stage, i.e., connected in series to L_{DM}. A DC-side or AC-side CM inductor is also advantageous for motor drive applications as it largely attenuates conducted CM emissions of unshielded motors cables and motor bearing currents [8].

topology and the conventional FPI-YI approach, and validate the proposed approach with a hardware demonstrator. The measured waveforms demonstrate sinusoidal output currents with the theorized reduction in LF peak and RMS current stresses of up to 90 % over the conventional FPI-YI topology.

This RPI-YI current stress reduction corresponds to an 80 % smaller magnetics volume, and harmonic injection techniques could further reduce the component stresses [5]. This concept is proposed and demonstrated for VSD systems, but is also applicable to buck-boost rectifier applications (cf., **Fig. 6**) that are equally important to our more-electric future.

REFERENCES

[1] "World energy outlook 2017," International Energy Agency (IEA), Nov. 2017. [Online]. Available: https://www.iea.org/reports/world-energy-outlook-2017

[2] "Energy efficiency - Motors and drives infographics (3AUA0000182864)," ABB, Dec. 2018. [Online]. Available: https://library.abb.com

[3] IEA, "Energy-efficiency policy opportunities for electric motor-driven systems," https://www.iea.org/reports/energy-efficiency-policy-opportunities-for-electric-motor-driven-systems, Paris, IEA Energy Papers 2011/07, May 2011.

[4] S. Nino, "Reversible buck-boost chopper circuit, and inverter circuit with the same," 2005, US Patent 7088595 B2. [Online]. Available: https://patents.google.com/patent/US7088595B2/en

[5] M. Antivachis, D. Bortis, L. Schrittwieser, and J. W. Kolar, "Three-phase buck-boost Y-inverter with wide DC input voltage range," in *Proc. of the IEEE Applied Power Electronics Conference and Exposition (APEC)*, Mar. 2018.

[6] M. Antivachis, D. Bortis, D. Menzi, and J. W. Kolar, "Comparative evaluation of Y-inverter against three-phase two-stage buck-boost DC-AC converter systems," in *Proc. of the IEEE International Power Electronics Conference (IPEC - ECCE Asia)*, May 2018, pp. 181–189.

[7] M. Antivachis, N. Kleynhans, and J. W. Kolar, "Three-phase sinusoidal output buck-boost GaN Y-inverter for advanced variable speed AC drives," *IEEE Journal of Emerging and Selected Topics in Power Electronics*, early access, Sep. 2020.

[8] D. Menzi, D. Bortis, and J. W. Kolar, "EMI filter design for a three-phase buck–boost Y-inverter VSD with unshielded motor cables considering IEC 61800-3 conducted and radiated emission limits," *IEEE Transactions on Power Electronics*, vol. 36, no. 11, pp. 12 919–12 937, 2021.

[9] A. Abdulslam and P. P. Mercier, "A passive-stacked third-order buck converter with inherent input filtering achieving 0.7W/mm^2 power density and 94% peak efficiency," *IEEE Solid-State Circuits Letters*, vol. 2, no. 11, pp. 240–243, 2019.

[10] Z. Du, B. Ozpineci, L. M. Tolbert, and J. N. Chiasson, "DC–AC cascaded H-bridge multilevel boost inverter with no inductors for electric/hybrid electric vehicle applications," *IEEE Transactions on Industry Applications*, vol. 45, no. 3, pp. 963–970, 2009.

[11] M. Pahlevaninezhad, P. Shangzhi, and P. Jain, "Zero voltage switching interleaved boost AC/DC converter," 2015, US Patent Application 20150194909 A1. [Online]. Available: https://patents.google.com/patent/US20150194909A1/en

[12] D. Rothmund, D. Bortis, J. Huber, D. Biadene, and J. W. Kolar, "10kV SiC-based bidirectional soft-switching single-phase AC/DC converter concept for medium-voltage solid-state transformers," in *Proc. of the IEEE International Symposium on Power Electronics for Distributed Generation Systems (PEDG)*, Apr. 2017, pp. 1–8.

[13] C. W. T. McLyman, *Magnetic core selection for transformers and inductors: a users's guide to practice and specification*. CRC Press, 1997.

[14] C. R. Sullivan, B. A. Reese, A. L. F. Stein, and P. A. Kyaw, "On size and magnetics: Why small efficient power inductors are rare," in *Proc. of the IEEE International Symposium on 3D Power Electronics Integration and Manufacturing (3D-PEIM)*, Jun. 2016, pp. 1–23.

[15] M. Hartmann, H. Ertl, and J. W. Kolar, "EMI filter design for a 1 MHz, 10 kW three-phase/level PWM rectifier," *IEEE Transactions on Power Electronics*, vol. 26, no. 4, pp. 1192–1204, 2011.

[16] J. Wang, Y. Zhang, M. Elshaer, W. Perdikakis, C. Yao, K. Zou, Z. Xu, and C. Chen, "Nonisolated electric vehicle chargers: Their current status and future challenges." *IEEE Electrification Magazine*, vol. 9, no. 2, pp. 23–33, 2021.